Chapter 4

Luminescence Characteristics of $Sr_3Al_2O_6:Tb^{3+}$ phosphor and Study of Energy Transfer between Tb^{3+} and Eu^{3+} in the $Sr_3Al_2O_6$ System

When you get a result that you expect, you have another result.
When you get a result that you don't expect, you have a discovery.
(Frank Westheimer)

4.1. Introduction

Recently, great emphasis has been given on the TL dosimetric properties of the display phosphor materials and the use of phosphor as an accidental dosemeter [1,2]. This has opened up new challenges to the researchers in this field. Accidental dosimetry has its applications in protecting humans as well as for the environment as a whole. Untill today the dosemetric materials mainly used for this purpose are $CaSO_4$:Dy and LiF:Mg, but a great deal of input and research has aided the development of phosphors doped with rare earths as well as the application of the lamp phosphors as dosemeters. This has lead to researchers of the field take notice and few of them have been reported in the work by Rosa et al [3,4,5] and Liu et al[6]. They have studied many of these phosphors and elaborated on the thermoluminescence properties and the applications of such as dosemeter. The dual nature of such phosphors has also been studied by Murthy et al [7,8]. Strontium aluminate, due to its long persistence property is one such material that has been studied extensively for almost a decade now [9,10]. In our earlier work we have reported the photoluminescence and thermoluminescence properties of rare earth doped, europium and dysprosium, $Sr_3Al_2O_6$ phosphor [11]. Not much has been written of the other $3SrO\text{-}Al_2O_3$ phase and its optical and thermoluminescent properties except its applicability as a mechanoluminscent material [12]. The TL phenomenon is the result of the interaction between ionizing and non-ionizing radiation with some material. In this chapter, the optical properties and thermoluminescent properties of $Sr_3Al_2O_6$ material doped with terbium is studied and elaborated. To study the effect of the beta irradiation on the nature and type of traps, and to understand the mechanism through which the radiative recombination is taking place, the thermoluminescence glow curves were recorded. The study discussed in this chapter has already been published in the journal paper [13]. For any phosphor to be a potential candidate as a dosimeter it should satisfy some set of parameters i.e. fading, linearity, reproducibility etc. [8]. All this dosimetric properties of the $Sr_3Al_2O_6$:Tb have been studied and discussed in detail in this chapter. The dopant concentration in the system was varied and the effect of concentration quenching was studied. The trap parameters have been evaluated by using Chen's equation. This chapter reports in length the analysis of the data and the effect of the beta irradiation on the terbium doped $Sr_3Al_2O_6$ phosphor.

Energy-transfer processes are very important in phosphor systems because they can cause an enhancement of the luminescence emission, but also they can greatly reduce it. This is usually achieved by the introduction of an ion of a different type, called a sensitizer or donor, into the laser host material in addition to the ion, called an activator or acceptor, which is responsible for the luminescence emission. The donor ion absorbs strongly at the pumping source energy, and transfers this excitation energy to the acceptor. The basic studies of energy transfer between Tb^{3+} and Eu^{3+} is observed and discussed in this chapter.

4.2. Experimental

4.2.1. Sample preparation

The synthesis of the $Sr_3Al_2O_6$ doped with different rare earths has been elaborated in the previous chapter-2. The phosphor samples were prepared by the reflux method. The starting materials taken were strontium nitrate and aluminium nitrate procured from S.D. Fine Chemicals, Mumbai, India with rare earths of purity 99.9%. The terbium oxide (Tb_4O_7) was converted to nitrate by mixing the rare earth in aqua regia solution and then slowly heating it. Thereafter the resulting powder was washed with concentrated nitric acid several times and was used as dopant in the present study. The samples were prepared by doping different concentration of terbium nitrate in the host matrix. The powders were weighed according to the nominal composition of $Sr(NO_3)_2$+$Al(NO_3)_3.9H_2O$+ x $Tb(NO_3)_3$ (where x = 0%, 0.25%, 0.5%, 1.0%, 1.5% and 2.0% respectively). The starting materials of strontium and aluminum nitrates were taken in stoichiometric ratio and dissolved in the appropriate amount of distilled water and kept for stirring. Thereafter the rare earth compound with different concentrations was mixed to the above solution. Citric acid and ethylene glycol were added to the solution after one hour of constant stirring. The resulting gel was set for refluxing at 80°C for 6 hours. The gel thus obtained, was kept for drying in an oven maintained at 100°C for 10 hours. The yellowish gel then transformed into a fluffy material. It was then kept for firing at a temperature maintained at 900°C in a furnace for 16 hours in air. The white powder obtained after firing, was ground using an agate mortar and pestle and was then subjected to various characterizations.

4.2.2. X-ray diffraction, Photoluminescence and Thermoluminescence Characterization

Phase identification of the powders was carried out by the X-ray powder diffraction using RIGAKU D'MAX III Diffractometer having Cu Kα radiation. The photoluminescence (emission and excitation spectra) were recorded at room temperature using spectrofluorophotometer RF-5301 of SHIMADZU make with a xenon source. The slit width of both the excitation and the emission monochromator was kept at 1.5nm and the sensitivity was kept as high for all the samples. The thermoluminescence glow curve of all the samples were recorded using Nucleonix make Thermoluminescence reader at a constant heating rate of 2.0°C/s. The amount of sample used for doing the TL was kept as 5mg and were then irradiated with Beta rays from a Sr-90 source of 50 mCurie strength.

High Temperature XRD: In the present case the instrument was a Philips X'pert Pro XRD unit equipped with Anton Paar HTK attachment. The high temperature sample holding stage used in this instrument consists of a platinum plate heated by platinum–rhodium heater for heating and recording of XRD of crystalline samples. The sample is spread over a platinum foil holder and the temperature of the platinum holder is controlled by a temperature controller. For lattice thermal expansion studies, XRD patterns of each sample was recorded from 2θ = 10 to 90°, in the temperature range 293 to 1473K on, at a regular interval of 200°C, in static air.

Room Temperature XRD: Powder XRD patterns were recorded on a Philips X-ray Diffractometer (PW 1710) with Ni filtered Cu K_α radiation and using silicon as an external standard. The measurements were performed in the range of 10° to 70° 2θ in a continuous scan mode with a step width of 0.02° and at a scan rate of 1° /min.

4.3. Result and Discussion

4.3.1. X-ray diffraction (XRD) studies

In order to determine the crystal structure, phase purity, chemical nature and homogeneity of the phosphors, X-ray diffraction (XRD) analysis was carried out. Figure 4.1. shows X-ray diffraction (XRD) pattern of the $Sr_3Al_2O_6:Tb^{3+}$ phosphor. From the XRD pattern analysis it was found that the prominent phase formed is $Sr_3Al_2O_6$. The $Sr_3Al_2O_6$ phase belongs to the space group pa3 having a cubic crystalline structure [14]. The traces of other phases like that of $SrAl_4O_7$ and $SrAl_2O_4$ peaks were weak. As the XRD patterns are

similar for all the terbium concentrations so only one with 1% terbium has been shown and it is also matching with that of the Kennedy et al. [15].

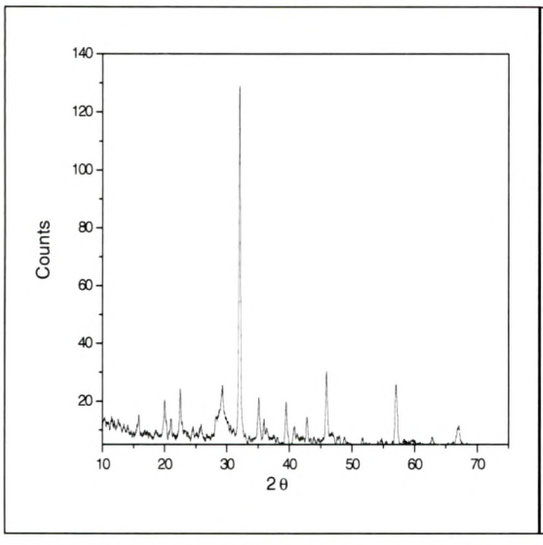

Figure 4.1. XRD pattern of $Sr_3Al_2O_6$:Tb (1%)

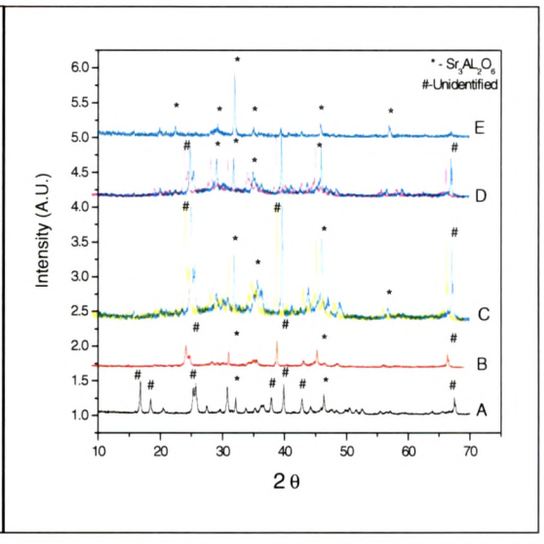

Figure 4.2. XRD pattern of $Sr_3Al_2O_6$:Tb (1%) measured at different annealing temperatures.
Curve A = 200 °C annealed phosphor;
B =400 °C annealed phosphor;
C = 600 °C annealed phosphor;
D = 800 °C annealed phosphor;
E = 900 °C annealed phosphor.

The luminescence characteristics of phosphor are strongly affected by the phase purity and crystallinity of particles. The effect of post treatment temperature on the crystal structure of prepared particles is shown in Figure 4.2. In this case, the $Sr_3Al_2O_6:Tb^{3+}$ phosphor particles were prepared from as per the method described in the experimental section. Then the XRD pattern of this phosphor was measured at different temperatures. The XRD pattern of this phosphor was measured at 200 ˚C, 400 ˚C, 600 ˚C, 800 ˚C and 900 ˚C as shown in Figure 4.2. represented by A, B, C, D, and E, respectively. As it can be observed from the HT-XRD patterns at different temperatures that at 200 ˚C there are lots of other unidentified phases present in the system including the starting materials $Sr(NO_3)_2$ and $Al(NO_3)_3$, but there is hardly any traces of $Sr_3Al_2O_6$ phase. The $Sr_3Al_2O_6$ phase started to form at 400 ˚C, but the percentage of starting materials and intermediate phases are higher. At 600 ˚C the $Sr_3Al_2O_6$ phase started to form as main phase and its main peak intensity also increases, but still there are some other intermediate phases are present. At 800 ˚C, the majority of $Sr_3Al_2O_6$ phase formation was observed and the peaks

of this phase were prominent, but there was also the existence of some intermediate phases. At 900 °C the phase pure XRD pattern of $Sr_3Al_2O_6$ was obtained without any traces of any other phase. Hence from this study we can conclude that the single phase $Sr_3Al_2O_6$ phosphor can be obtained at 900 °C when it was synthesized by reflux sol-gel technique.

4.3.2. Photoluminescence (PL) Characteristics

The emission and excitation spectra were recorded at room temperature for the $Sr_{3-x}Al_2O_6$: xTb^{3+} (where x= 0.025%, 0.1%, 0.5%, 1.0%, 1.5% and 2.0%) sample and are shown in Figure 4.3. A and B, respectively. The emission spectra show the peaks mainly at 489nm, 545nm, 585nm and 620nm respectively when excited with 254nm. These have been identified as due to the transitions $^5D_4 \rightarrow {}^7F_{6,\ 5,\ 4\ \text{and}\ 3}$ and related to the trivalent terbium ions in the $Sr_3Al_2O_6$ phosphors. Of these, the green emission at 545nm ($^5D_4 \rightarrow {}^7F_5$) is more intense than all the other transitions. It is a magnetic dipole transition with J = ± 1 displaying a bright green emission [16].

This can also be attributed to the fact that even for higher concentration of terbium in the host matrix, the absence of blue emission was typical as the cross relaxation produces an increase in the population of the $^5D_4$ state at the expense of the $^5D_3$ state [17]. Moreover, we found that as the concentration of the terbium was increased in the host lattice, there was a significant increase in the intensity of all the terbium transitions and at 2.0 mol% terbium concentration the observed intensity for 545nm i.e. $^5D_4 \rightarrow {}^7F_5$ was out of range of the measuring instrument. The excitation spectra show the peak at 254nm when monitored with 545nm. This is a broad band starting from 220nm and ending at around 290nm. The intensity of this band goes on increasing as the concentration increases from 0.025% to 2.0% and it was also recorded out of range of the measuring instrument for the terbium concentration at 2%. This is in agreement with the same result for the emission too and they both follow the same pattern. The peak at 254nm signifies that this has a potential to be used as a green emitting phosphor in CFL and fluorescent lamps.

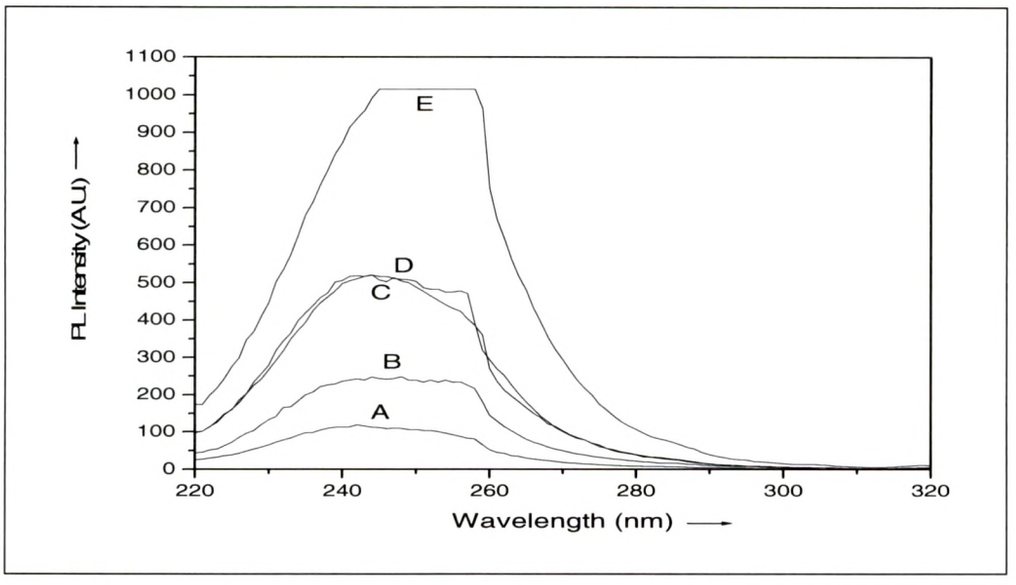

Figure 4.3.A. Excitation spectra of $Sr_3Al_2O_6:Tb^{3+}$. Emission: 545nm.
Curve A= 0.025%Tb; B= 0.1%Tb; C= 0.5%Tb; D= 1%Tb; E = 2%Tb.

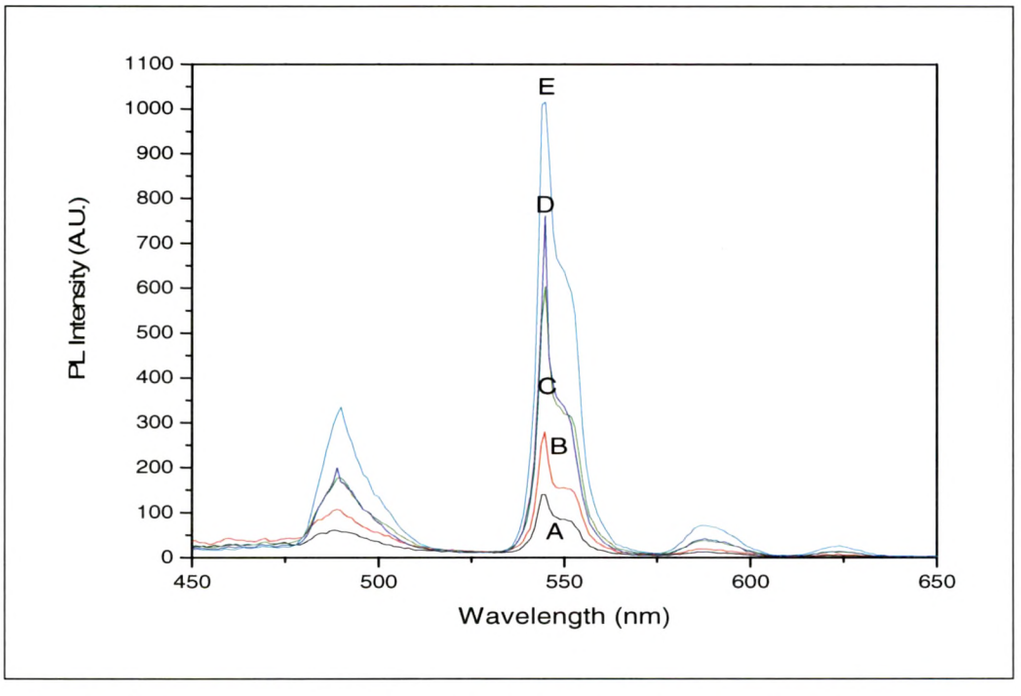

Figure 4.3.B. Emission spectra of $Sr_3Al_2O_6:Tb^{3+}$. Excitation: 254nm.
Curve A= 0.025%Tb; B= 0.1%Tb; C= 0.5%Tb; D= 1%Tb; E = 2%Tb.

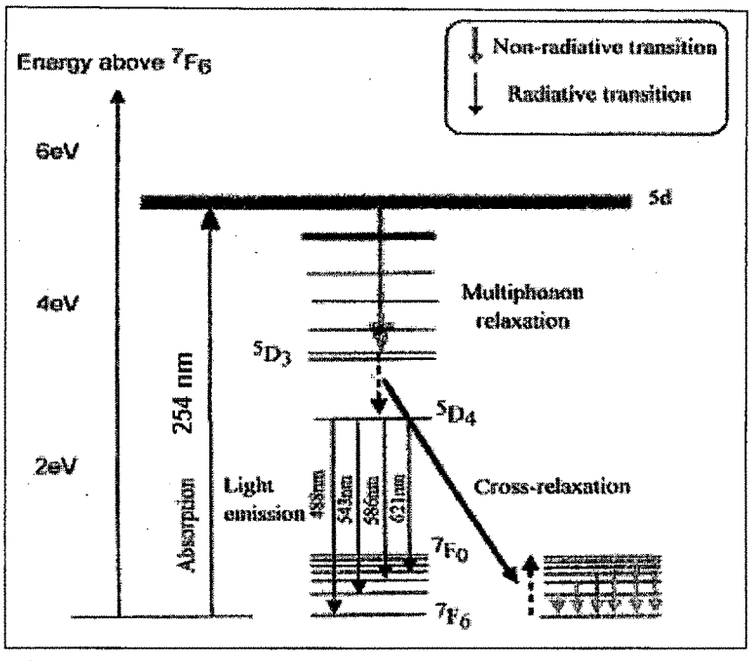

Figure 4.4. Energy diagram for Tb^{3+} ion in the $Sr_3Al_2O_6$ system.

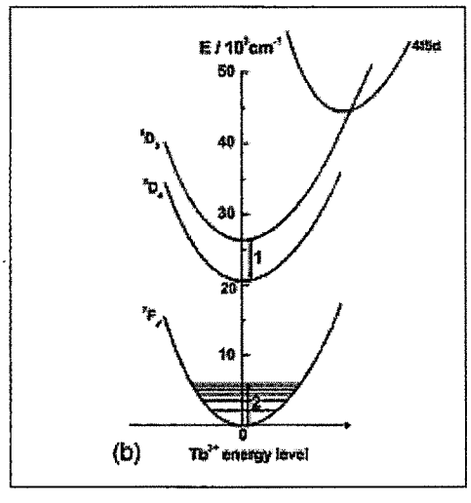

Figure 4.5. Schematic configurational coordinate diagram for Tb^{3+} in $Sr_3Al_2O_6$ showing quenching of the higher level emission by cross-relaxation: the $^5D_3$ emission on ion 1 is quenched by transferring the energy difference $^5D_3$–$^5D_4$ to ion 2 which is promoted to $^7F_0$ level.

Table 4.1: PL emission intensity of $Sr_3Al_2O_6:Tb^{3+}$ for varying Tb^{3+} concentration.

Sample Code	Tb^{3+} Concenctration	Peak intensity for 490 nm (A.U.)	Peak Intensity for 545 nm (A.U.)
A	0.025%	6.60	146
B	0.1%	106	275
C	0.5%	160	590
D	1%	191	755
E	2%	340	Out of range (~1023)

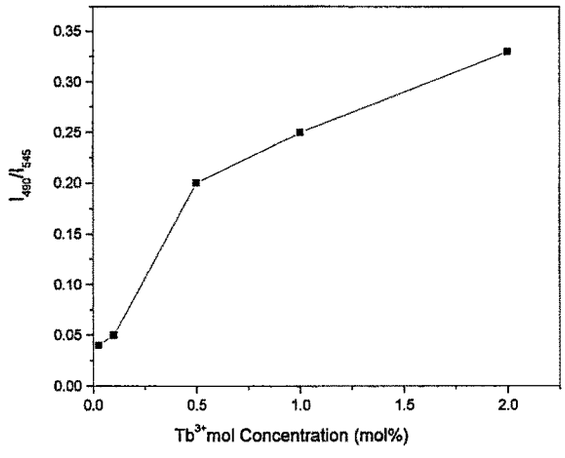

Figure 4.6. Variation of the peak ratio (I_{490nm}/I_{545nm}) with terbium concentration (mol%) of $Sr_3Al_2O_6$ from photoluminescence measurements.

The energy band diagram of the terbium optical transitions is shown in Figure 4.4. Under optical excitation an electron is promoted to a 5d localised band. The excited electron then non-radiatively relaxes to the $^5D_3$ energy level [18]. As Tb^{3+} concentration is high and the $^5D_3 \rightarrow ^5D_4$ transition is resonant with the $^7F_6 \rightarrow ^7F_{0,1}$ transition the energy from the $^5D_3 \rightarrow ^7D_4$ transition may be taken up by a neighbouring ion via a cross-relaxation process [19]. The observed green emission is caused by the $^5D_4 \rightarrow ^7F_{n=3,4,5,6}$ transitions indicated in the figure. For these transitions to be quenched in any particular Tb^{3+} ion by surrounding Tb^{3+} ions (concentration quenching) requires that at least two neighbours are excited to a specific energy state. The probability that this non-radiative decay will occur is extremely low and has been found to be experimentally unimportant [20]. Any luminescence quenching in terbium oxide then occurs via excitation transfer to non-radiative sinks, such as defects or impurities. This may occur as a result of either direct energy transfer to acceptor states or by migration of the excitation among Tb^{3+} ions until it arrives in the vicinity of a suitable sink [21]. One can also observe from the Figure 4.6.

that as the concentration of Tb^{3+} increases the ratio between the intensities of 490 nm and 545 nm increases.

4.4.Thermoluminescence (TL) Characteristics

The Thermoluminescence response of the terbium doped $Sr_3Al_2O_6$ phosphor has been studied above room temperature. Uptill now, the TL study of the SrO- Al_2O_3 system was done only to find out the kinetic parameters of the phosphor so as to find the trap depth responsible for the persistence of the phosphor as the traps lie at a lower temperature region [22]. As per our knowledge the application of the SrO-Al_2O_3 system as a dosimeter is new concept which has not been studied yet. The TL measurement of $Sr_3Al_2O_6$: Tb (1%) were carried out to ascertain the defects present in the synthesized compound. By considering the high radiation field during a nuclear disaster, a test dose of 100 Gy from a beta source (Sr-90) was given to the samples. The thermoluminescence glow curve of the $Sr_3Al_2O_6:Tb^{3+}$ (1%) sample was obtained in the temperature range between room temperature to 450°C. The TL glow curve of the $Sr_3Al_2O_6:Tb^{3+}$ (1%) phosphor is shown in Figure 4.7. The first peak at 124°C along with a hump at around 163°C and a second peak at around 350°C was observed.

4.4.1. Separation of TL peaks by T_{stop}-Method

To isolate the complicated and forbidden peaks of the glow curve the "Thermal Cleaning" technique [23] was applied. To separate the hump from the 124°C peak, the fresh sample was exposed to beta rays for same time to accumulate equal dose. The irradiated material was then heated upto 122°C to bleach or clean the 124°C peak. TL was again recorded under the same conditions. The hump at 163°C emerged as a single peak. To find out the existence of more forbidden peaks at and above this temperature, the procedure of thermal cleaning was repeated after every 10°C. But no other peak was observed except the peak at 350°C.

The analysis of all the three isolated glow peaks was done in order to evaluate the kinetic parameters such as trap depth and order of kinetics. Of the different methods described in the literature [24] for the analysis of the glow curves, the peak shape method was used for evaluation, as this is the most widely used and accepted for the glow curve parameters analysis. The order of kinetics of all the glow curves was calculated by measuring the symmetry (geometrical, μ_g) factor:

$$\mu_g = \delta/\omega \text{ ----------(1)}$$

The values of the δ, ω and τ were calculated as follows:-

$\delta = T_2 - T_m$, The high-temperature half width of the glow curve.

$\omega = T_2 - T_1$, The full width of the glow peak at its half height.

$\tau = T_m - T_1$, The low- temperature half width of the glow curve.

From the values of the geometrical factor it is clear that all the three peaks obey General Order Kinetics. The trap depth or the activation energy was calculated by using the Chen's equation [24]:

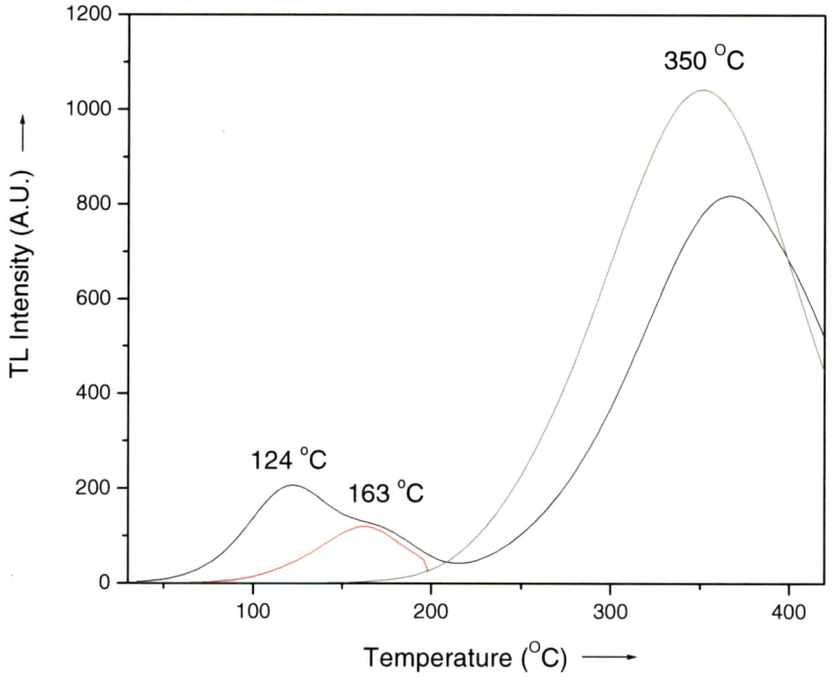

Figure 4.7. TL spectra 1% Tb. Dashed and doted line shows the different peaks separated after performing the T-stop method.

$$E_\alpha = c_\alpha(kT_m^2/\upsilon) - b_\alpha(2kT_m) \text{----------(2)}$$

Where k = Boltzmann constant, T_m = Peak Temperature

The value of the constants, c_α & b_α was calculated by the Chen's Equation for the General Order Kinetics. Where α was replaced by δ, ω or τ as the case may be.

Table 4.2: The list of calculated values by the Chen's equation.

Peak Temperature T_m (°C)	Geometrical Factor (μ_g)	E_τ (ev)	E_ω (ev)	E_δ (ev)	Mean E (ev)
124	0.55	0.75	0.75	0.746	0.748
163	0.5	0.77	0.79	0.81	0.79
350	0.475	0.65	0.71	0.77	0.71

It is clear from the calculated trap depth of the $Sr_3Al_2O_6$: Tb^{3+} (1%) phosphor that the values are too deep to give phosphorescence at room temperature. The mean activation energy for the temperature region at 124 °C comes out to be 0.748 eV and for the 163 °C it comes out be 0.79 eV. The addition of the terbium as activator produces deep traps at temperature around 120 to 350 °C which could be useful for dosimetric purpose due to their thermal stability and low fading. The role of the dopant in the host matrix is to increase the overall oxygen vacancies and in consequence number of trapped charge carriers that in turn induce an increment of the TL signal intensity. The glow peaks of the phosphor indicates that the presence of the terbium ions increases the TL efficiency by increasing the number of trapping charge carriers and the radiative recombination efficiency of those freed electrons or holes by thermally stimulating them. Evidently, the dopant ion increases the defect formation that promotes the trapping and recombination processes [5].

To observe the effect of the activator concentration on the TL glow curve of $Sr_3Al_2O_6$: Tb^{3+} phosphor, the TL of the samples of different terbium concentration under the same dose were recorded and are presented in Figure 4.8. The increase in the peaks intensity with respect to concentration of terbium upto 0.5 mol%, is an indication that the corresponding charge carrier traps are produced by the oxygen vacancies [4]; similarly the decrease in the TL intensity after 0.5 mol% of terbium concentration is attributed to the reduction of oxygen vacancies i.e. no additional traps were created at higher concentration of Tb^{3+} [5].

4.4.2. Effect of different Terbium concentration on TL glow curve

The shapes of all the glow peaks remain constant in the concentration range studied. As shown in the inset of the Figure 4.8., the TL output of the sample firstly increases with increasing concentration of terbium from 0.25mol% to 0.5mol%, reaches the maximum value at 0.5 mol % and then gradually decreases from 1 mol% to 2 mol%. This is a well

known concentration quenching phenomenon which was also observed for $Ba_2Ca(BO_3)_2$:Tb [6], $CaSO_4$:Dy [25]. The percent of the signal remained at 2 mol% for peaks 124 ˚C, 163 ˚C and 350 ˚C are ~6%, ~6% and ~ 38 %, respectively. That means the increase in the mol concentration mainly affects to the low temperature peak as well as the dosimetric peak. Whereas the peak at 350 ˚C is hardly shows much decrease in the TL intensity after increasing the concentration of the terbium ion.

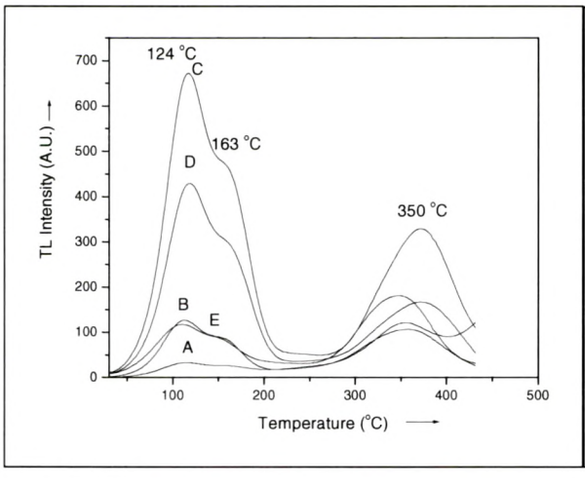

Figure 4.8.A. TL glow curves of $Sr_3Al_2O_6$:Tb phosphor with different Tb^{3+} concentrations irradiated with a 100 Gy β dose at room temperature, where A = 0.025%, B = 0.1%, C = 0.5%, D = 1.0%, E = 2.0%.

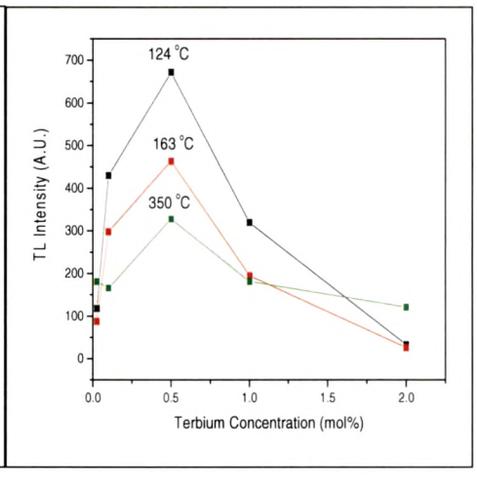

Figure: 4.8.B. Integrated TL intensity for different Tb concentrations for respective peak temperatures. Dose = 100 Gy.

Table 4.3: TL peak intensity of $Sr_3Al_2O_6$:Tb^{3+} phosphor for varying Tb^{3+} concentration

Sample Code	Tb^{3+} Concentration	Intensity of the Peak 124 ˚C (A.U.)	Intensity of the Peak 163 ˚C (A.U.)	Intensity of the Peak 350 ˚C (A.U.)
A	0.025%	32	26	122
B	0.1%	116	80	107
C	0.5%	649	457	301
D	1%	420	295	156
E	2%	108	76	179

4.4.3. Fading Effect of $Sr_3Al_2O_6$:Tb (1%) phosphor

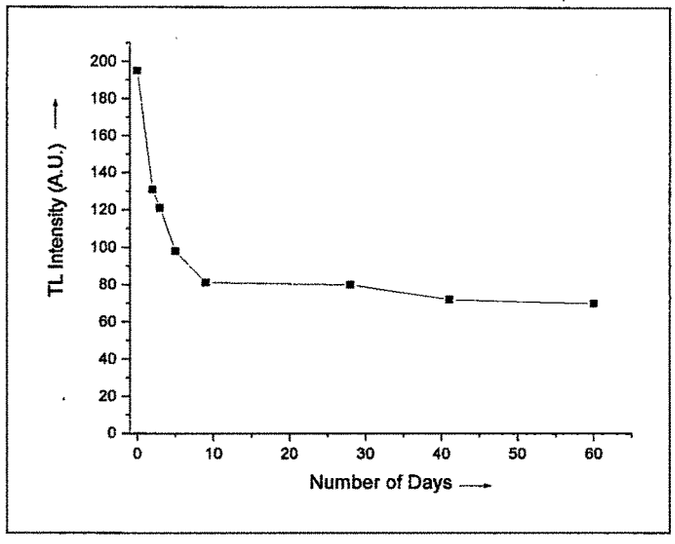

Figure 4.9. Fading effect of $Sr_3Al_2O_6$:Tb (1%) observed for 60 days.

For sample to be useful in dosimetry, the TL intensity of its dosimetric peaks should be stable and no fading should be observed when stored for long period after exposure. In order to investigate the fading characteristics of peak 1 and 2, the phosphor samples were stored in dark conditions at room temperatures between 25 and 30 °C over a period of two months after beta 100 Gy exposures. Figure 4.9. shows the plot of integrated TL counts vs. number of days of fading experiment. The result demonstrated a very intense decrease of the TL response during the first 24 hours of the time in the main peaks. It is seen that the first peak at 124 °C fades completely after one day or 24 hours of irradiation hence it has no dosimetric value. So, the influence of this peak in dosimetric measurements can be easily eliminated by making the TL measurements after a post-irradiation pre-read anneal at about 100 °C for few seconds in the TL reader system. The fading effect of beta irradiated sample is due to the recombination of the trapped electrons which can be released at room temperature. To study the fading effect, the phosphor $Sr_3Al_2O_6$:Tb(1%) was given the test dose of 100Gy from Sr-90 β source and the TL signal was recorded at different time interval for nearly two months. Figure 4.9. depicts the plot between TL intensity versus number of days after exposure. Strong fading was observed after 10 days of irradiation, as the phosphor $Sr_3Al_2O_6$:Tb (1%) lost around 59% of the TL signal when compared with the as irradiated sample. But after this, the decay is quite slow and finally stabilizes after 1 month or 30 days. The 41% remnant TL signal is higher enough to be considered for dosimetric applications [3,13]. The 124 °C peak slowly disappears after

one day and the hump at 163 °C turns into a well-defined peak, hence for TL dosimetric purpose the peak/hump at 163 °C was taken into consideration and studied. The activation energy for both the traps are very near to each other (from Table 1) so the chances of the charge transfer from the lower to higher temperature region i.e. at 163 °C are brighter, hence increasing the population of the active charges at the higher region. In order to minimize the fading of TL, it is advisable to anneal the phosphor to 120 °C for 3min, so that the unstable 120 °C peak get erased and the main dosimetric peak 163 °C will not be affected due to this low temperature fading. This method is generally used for all dosimetric phosphors.

4.4.4. Dose response of $Sr_3Al_2O_6$:Tb (1%) phosphor

The dose response of $Sr_3Al_2O_6$:Tb were studied as a function of irradiation between 25 Gy to 450 Gy using beta rays. Figure 4.10. A shows some of the selected glow curves of terbium doped samples at different dose levels. Samples were read immediately after irradiation. It is seen that there are no great differences in the glow curve structure of samples with increasing dose levels. As seen from figure 4.10. A, the main glow peaks of the sample i.e. the peak at 163 °C, were increases linearly with increasing beta ray dose up to 450 Gy and no saturation trend is observed in them up to the applied maximum dose levels. It should be mentioned that the intensity of the peak at 350 °C in $Sr_3Al_2O_6$:Tb phosphor also increases linearly but due to its spurious behaviour we have not taken this peak into TL dosimetric consideration. These results were obtained from the peak height measurements but the peak area measurements were also given similar results. So, in contrast to other common TL materials, $Sr_3Al_2O_6$:Tb compounds show extremely useful TL feature of perfect linearity in its TL response with dose upto 450 Gy. Generally, supralinearity is a characteristic of a large variety of TL materials, so TL linearity in the high dose region, over 10 Gy, is exceptionally rare. The linear relationship with TL intensity and absorbed dose is another desirable property of a TL dosimeter. It can be observed that the phosphor does not loose its linearity even at high doses of irradiation.

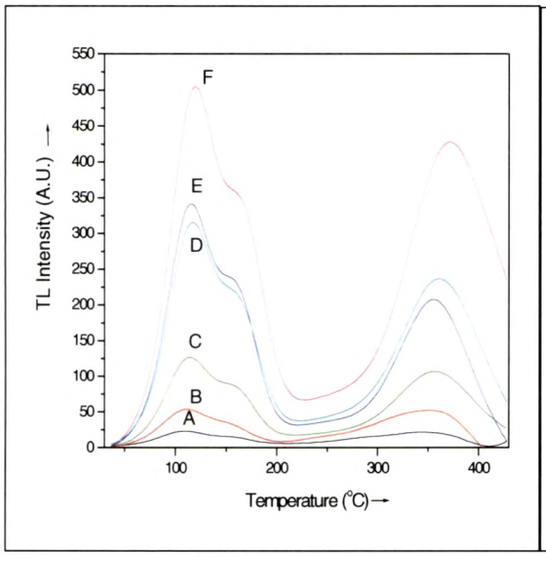

Figure 4.10.A. Study of dose response $Sr_3Al_2O_6$:Tb (1%) with the TL intensity and it is linear for the dose range between 1Gy to 450Gy of Sr-90. Curve A = 25 Gy; B = 75 Gy; C = 150 Gy; D = 225 Gy; E = 300 Gy; F = 450 Gy.

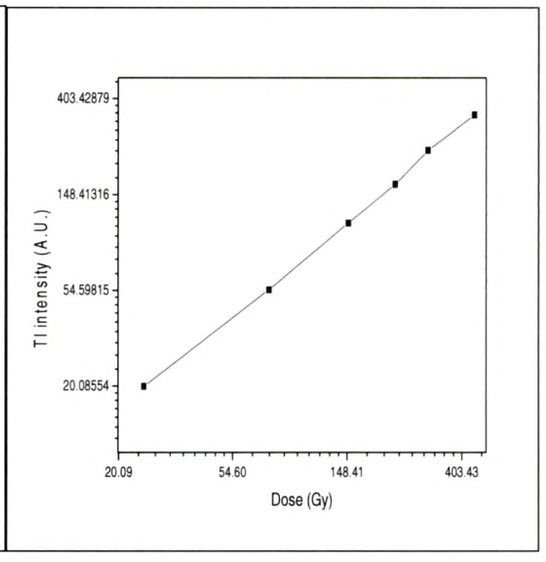

Figure 4.10.B. The dose response with respect to TL Intensity for 163 °C peak in the log scale.

4.4.5. Measurements of reproducibility in TL readouts

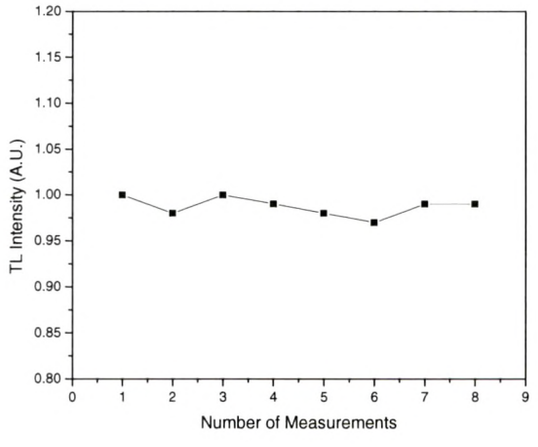

Figure 4.11. The reproducibility of a $Sr_3Al_2O_6$:Tb (1%) for a number of TL readouts.

In order to assess the reproducibility of the dose measurements attainable using $Sr_3Al_2O_6$:Tb sample, the TL stability after repeated cycles were measured. The reusability is another useful property of the dosimetric phosphor. If the sensitivity of the sample does not change after several cycles of exposure and readouts, then it is considered to be as a

good dosimetric phosphor. The $Sr_3Al_2O_6$:Tb (1%) was also tested for its reusability, the sample was exposed to beta rays for 100Gy and the TL glow curve was recorded from room temperature to 450 °C. It was then quickly cooled to room temperature and exposed to 100Gy from Sr-90 source to accumulate the dose. The glow curve was again recorded for the second time; several such cycles of exposures and glow curve recordings were performed and are shown in Figure 4.11. No significant change in the intensity of both the 120 °C and 164 °C peaks was observed. Excellent reusability is thus seen in the present sample and mainly for the peak in consideration at 164 °C. The results showed that reproducibility is well maintained within less than 1% based on standard deviation over more than 8 repeated cycles for the dose of 100 Gy beta irradiation.

4.4.6. Discussion of 350 °C TL peak

The peak at around 350 °C was related to the phenomenon known as spurious TL i.e. glow curve which does not result from the irradiation of the specimen. There are many possibilities of such spurious glow such as [23]:

(i) Due to the transfer of charge from the deep trap to the dosimetry traps during exposure to light.

(ii) Tribothermoluminescence can be another factor which can contribute, where the trapping of the charge in the TL traps follow mechanical effect upon the specimen (friction, grinding etc.)

(iii) Due to chemiluminescence produced during the read out (probably due to the oxidation of the surface impurities).

Although the presence of this spurious signal does not show any effect on the dosimetric peak which was studied at 163 °C. The reliability of the 163 °C peak is also not disturbed due to this spurious signal. Though there can also be a possibility of the role of impurity present in the sample at ppm level and also due to the high temperature synthesis as also observed by Chatterjee, et al for Gd_2O_2S:Tb phosphor [26]. The third peak at 350 °C was at higher temperature region so the activation energy for it was not calculated and emphasis was given only to the other two peaks at 124 °C and 163 °C.

4.5. Energy transfer between Tb^{3+} and Eu^{3+} in the $Sr_3Al_2O_6$ system

The process of transferring the excitation energy from donor to acceptor is called energy transfer. The center, which absorbs and transfers energy is called the sensitizer and the center to which the absorbed energy transferred to is called activator. Energy transfer can occur between two identical luminescent centers or between two non-identical centers. According to the theory of energy transfer developed by Förster (1948) and later by Dexter (1953) the efficiency of energy transfer [27] depends mainly on the extent of spectral overlap between the absorption band of acceptor and emission band of donor with the suitable interaction between them [28]. Energy transfer from a sensitizer to an activator may take place either via radiative transfer or non-radiative transfer through exchange interaction or electric multipole interaction. As a result of energy transfer the luminescence properties of a pair of ions can be different from that of the single ions. Often, energy transfer in terms of multipolar interactions between two ions is used for the sensitization of one of the ions to achieve brighter emissions [29].

4.5.1. Photoluminescence emission spectra of $Sr_3Al_2O_6:Tb^{3+},Eu^{3+}$ phosphor

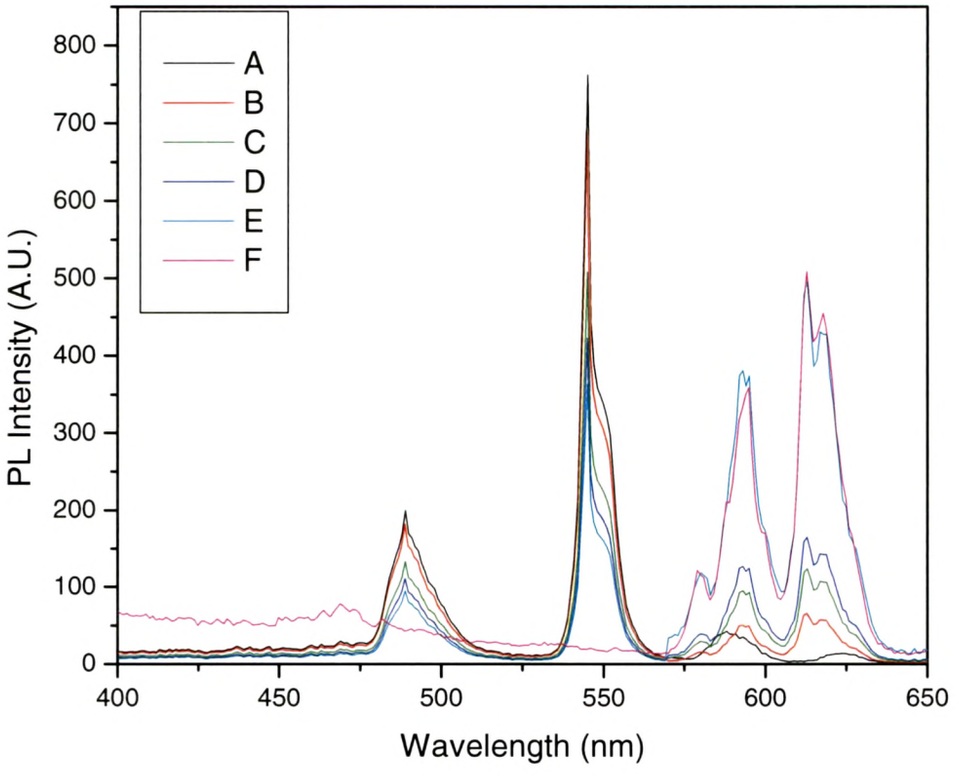

Figure 4.12. Emission chracterisitcs of $Sr_3Al_2O_6$:Tb(1%),Eu(x%).
Curve A = $Sr_3Al_2O_6$: Tb(1%);
B = $Sr_3Al_2O_6$:Tb(1%),Eu(0.025%);
C = $Sr_3Al_2O_6$:Tb(1%),Eu(0.1%);
D = $Sr_3Al_2O_6$:Tb(1%),Eu(0.5%);
E = $Sr_3Al_2O_6$:Tb(1%),Eu(1%);
F = $Sr_3Al_2O_6$:Eu(1%).

Table 4.4: Photoluminescence (PL) peak intensity of $Sr_3Al_2O_6$:Tb,Eu for varying concentration of Eu^{3+}.

Sample Code	$Sr_3Al_2O_6$: Tb(x), Eu(y)	Intensity of 545nm (A.U.)	Intensity of 592nm (A.U.)	Intensity of 613nm (A.U.)
A	$Sr_3Al_2O_6$: Tb(1%)	762	35	4
B	$Sr_3Al_2O_6$:Tb(1%),Eu(0.025%)	693	51	47
C	$Sr_3Al_2O_6$:Tb(1%),Eu(0.1%)	508	95	87
D	$Sr_3Al_2O_6$:Tb(1%),Eu(0.5%)	423	127	116
E	$Sr_3Al_2O_6$:Tb(1%),Eu(1%)	362	381	349
F	$Sr_3Al_2O_6$:Eu(1%)	20	360	510

Figure 4.12. shows the excitation spectra of the $Sr_3Al_2O_6$:Tb, Eu system when excited with the 254nm wavelength. The curve A shows the shows the emission pattern of Tb^{3+} (1%) only having narrow band emission at 489, 545, 585 and 625 nm for the characteristic transition of $^5D_4 \rightarrow {}^7F_{J=6,5,4,3}$ respectively. Curve B shows the emission spectra of $Sr_3Al_2O_6$:Tb(1%),Eu(0.025%). The intensity of the terbium emission band decreases slightly and the characteristic emission of trivalent Eu^{3+} is observed at 580 nm, 592 nm, 595 nm, 613 nm, 617 nm ascribed to the transition $^5D_0 \rightarrow {}^7F_J$ (J = 0, 1, 2). Hence there is an energy transfer occurs between Tb^{3+} and Eu^{3+} ions in the host lattice. To observe further the energy transfer phenomenon we slowly increased the concentration of the Eu^{3+} in the system by keeping the concentration of terbium constant i.e. 1%. The concentration of europium was increased from 0.025% to 1%. The emission spectra of this double doped system signifies that the emission intensity of terbium decreases nonlinearly and Eu^{3+} increases linearly with europium concentration. The emission spectra of $Sr_3Al_2O_6$:Tb(1%), Eu(1%) shows that the a beautiful yellow emission can be obtained from this phosphor when excited with the ultraviolet wavelength.

Figure 4.13. and 4.14 represents the energy level diagram of all the possible transitions of Tb^{3+} and Eu^{3+} doped system. Out of all these emissions we observed only emissions shown in Figure 4.12. The $^5D_3$ transition of Tb^{3+} is already absent due to the cross relaxation at higher concentration and the Eu^{3+} shows only the transition $^5D_0 \rightarrow {}^7F_J$ (J = 0, 1, 2).

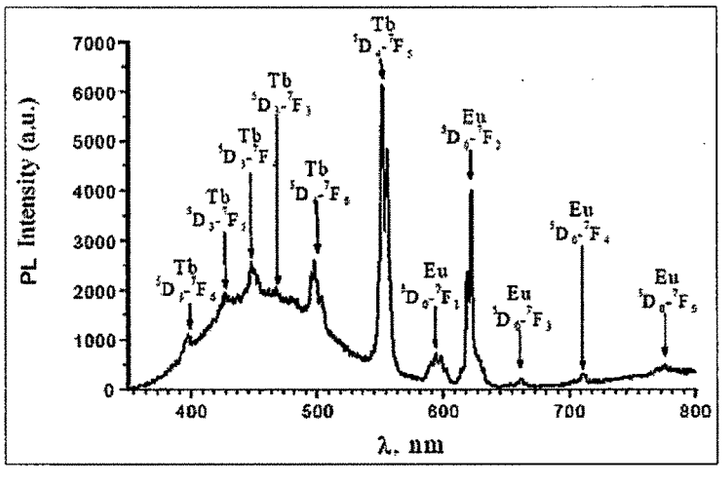

Figure 4.13. PL spectra of $Sr_3Al_2O_6$, activated with the trivalent ions of Tb^{3+} and Eu^{3+}.

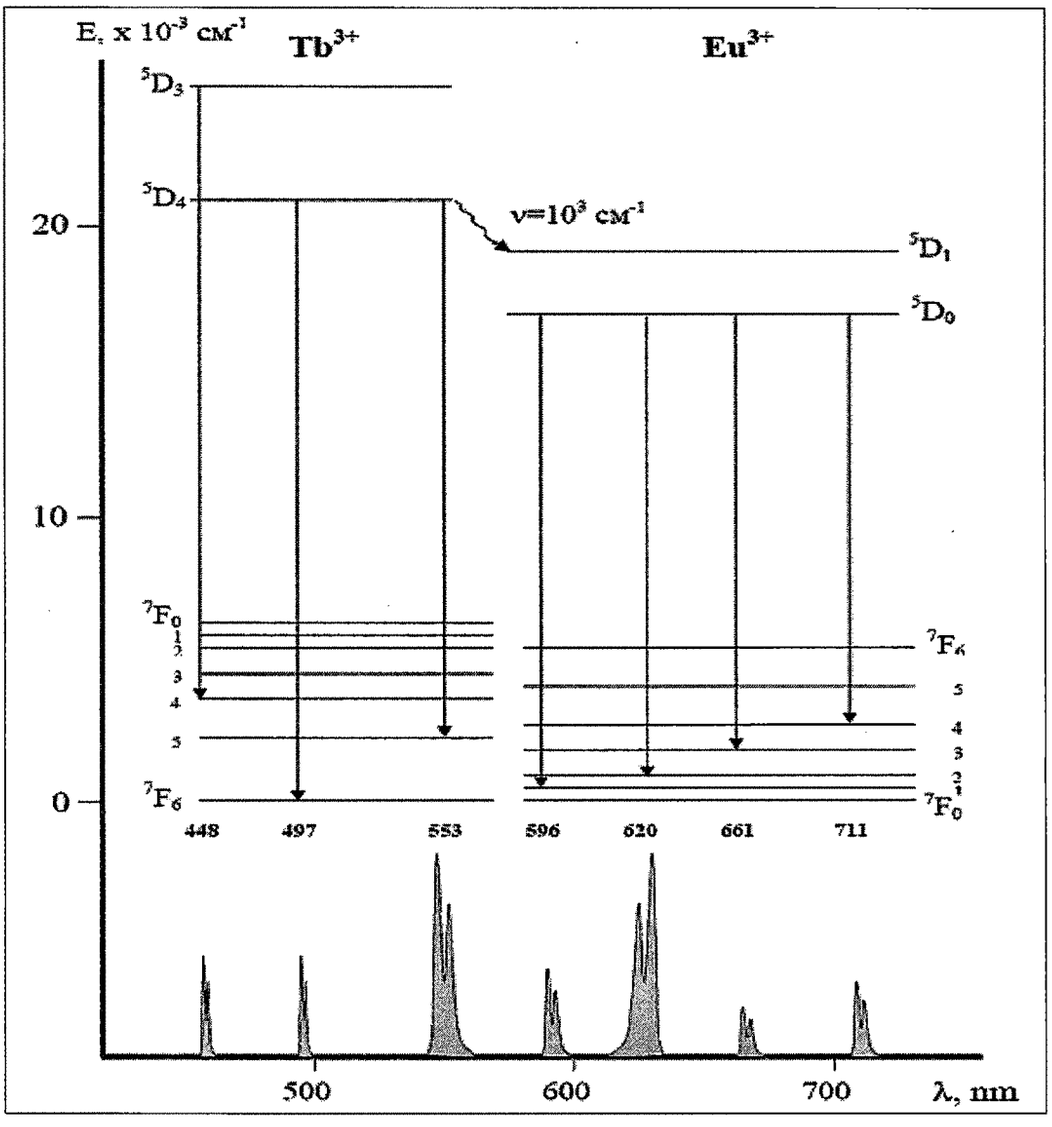

Figure 4.14. Schematic representation of the energy transfer in $Sr_3Al_2O_6$, activated with the trivalent ions of Tb^{3+} and Eu^{3+}.

4.5.2. Photoluminescence excitation spectra of $Sr_3Al_2O_6:Tb^{3+},Eu^{3+}$ phosphor

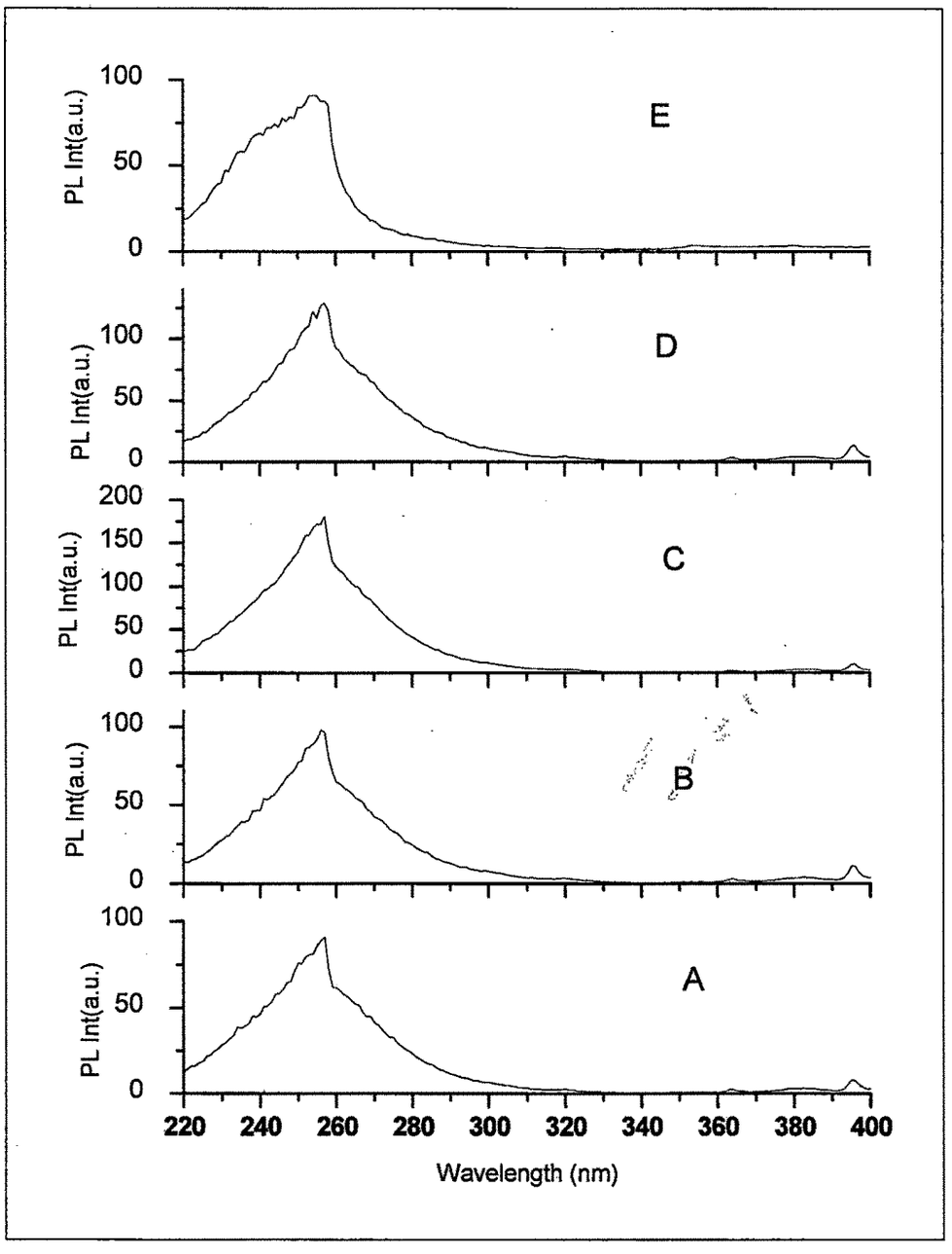

Figure 4.15. Excitation spectra of $Sr_3Al_2O_6:Tb^{3+},Eu^{3+}$.
Curve A = $Sr_3Al_2O_6$:Tb(0.1%),Eu(1%);
B = $Sr_3Al_2O_6$:Tb(1%),Eu(0.5%);
C = $Sr_3Al_2O_6$:Tb(0.025%),Eu(1%);
D = $Sr_3Al_2O_6$:Tb(0.5%),Eu(1%);
E = $Sr_3Al_2O_6$:Tb(0.025%),Eu(0.025%)

Table 4.5: PL excitation peak intensity of $Sr_3Al_2O_6$:Tb,Eu for varying concentration of Tb^{3+} and Eu^{3+}.

Sample Code	$Sr_3Al_2O_6$:Tb(x),Eu(y)	PL Intensity of 254nm peak (A.U.)	PL Intensity of 395nm peak (A.U.)
A	$Sr_3Al_2O_6$:Tb(0.1%),Eu(1%)	90	10
B	$Sr_3Al_2O_6$:Tb(1%),Eu(0.5%)	97	11
C	$Sr_3Al_2O_6$:Tb(0.025%),Eu(1%)	177	14
D	$Sr_3Al_2O_6$:Tb(0.5%),Eu(1%)	128	12
E	$Sr_3Al_2O_6$:Tb(0.025%),Eu(0.025%)	92	-

Figure 4.15 shows the excitation spectra of the $Sr_3Al_2O_6$:Tb, Eu phosphor measured at different emission wavelengths for the respective concentration of Tb^{3+} and Eu^{3+}.

For $Sr_3Al_2O_6$:Tb (0.025%), Eu (0.025%) the excitation spectra was measured for 594 nm.

The excitation band show peak around 254 nm which shows the emission is due to the transition of charge transfer band for the system.

$Sr_3Al_2O_6$: Tb (0.5%), Eu (0.1%) shows the sharp excitation at 254 nm which show a small split at 253 nm when measured for the emission wavelength 545 nm.

The excitation peak of $Sr_3Al_2O_6$: Tb (0.025%), Eu (1%); $Sr_3Al_2O_6$:Tb(1%), Eu (0.5%); and $Sr_3Al_2O_6$:Tb (0.1%), Eu (1%) shows the band around 254 nm. One can observe that except for the $Sr_3Al_2O_6$:Tb(0.025%), Eu (0.025%) system, all the systems shows a excitation peak at around 490nm, which corresponds to the Eu^{3+} transitions. The presence of this peak is the evidence of the energy transfer from Tb^{3+} to Eu^{3+} in this system.

4.5.3. Photoluminescence emission spectra of $Sr_3Al_2O_6:Tb^{3+},Eu^{3+}$ phosphor with varying concentration of Tb^{3+} and Eu^{3+}

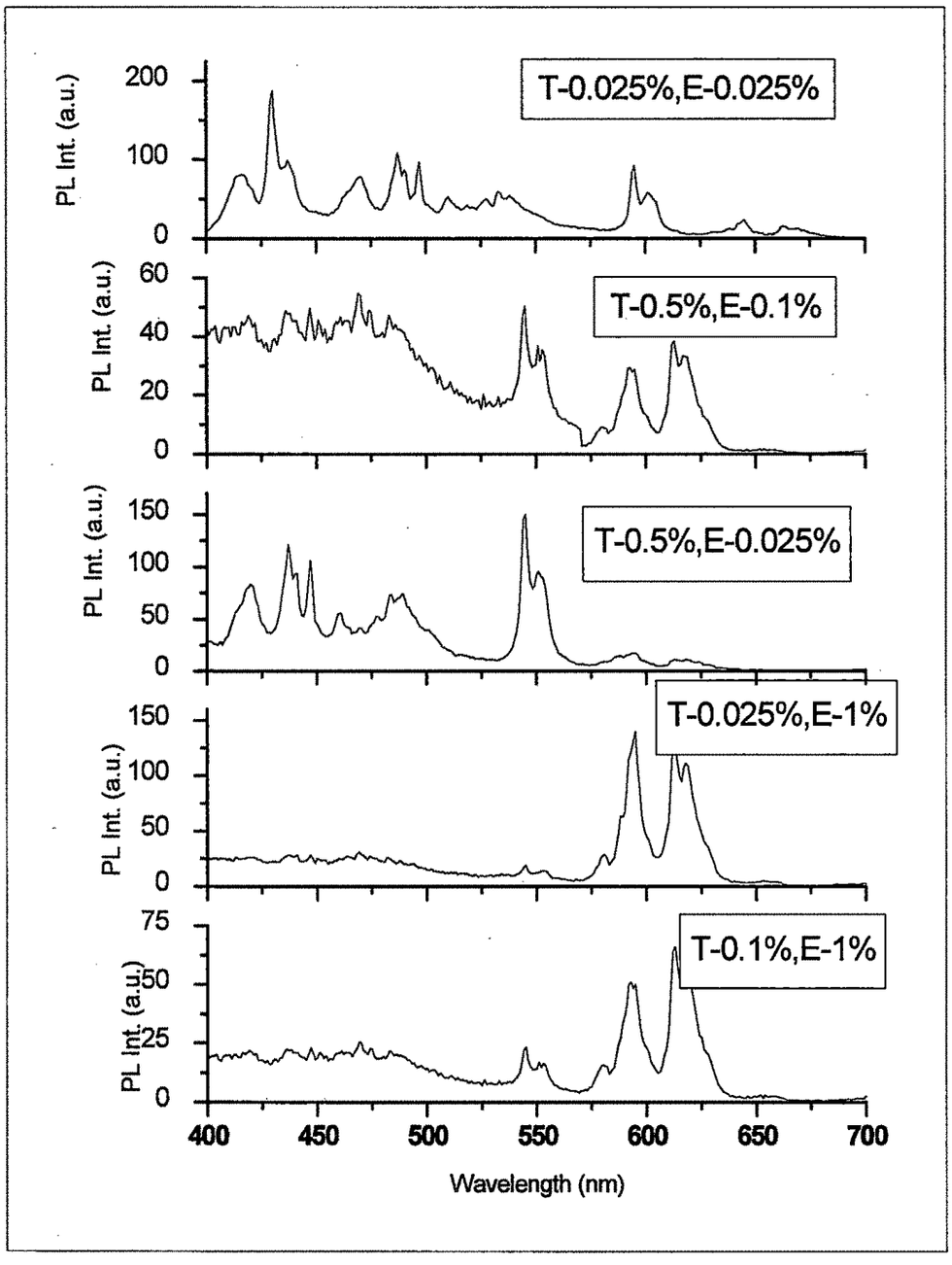

Figure 4.16. Emission spectra of $Sr_3Al_2O_6:Tb^{3+}$, Eu^{3+} measured for varying concentration of Tb^{3+} and Eu^{3+} as indicated in the figures. Where T = Tb^{3+} and E = Eu^{3+}.

Table 4.6: PL emission peak intensity of $Sr_3Al_2O_6$:Tb,Eu for varying concentration of Tb^{3+} and Eu^{3+}.

Sample Code	$Sr_3Al_2O_6$:Tb(x),Eu(y)	PL peaks observed on wavelengths (nm)	PL peak intensity for the respective wavelengths (A.U.)
A	$Sr_3Al_2O_6$:Tb(0.1%),Eu(1%)	544, 551, 593, 611, 617	21, 16, 48, 64, 57
B	$Sr_3Al_2O_6$:Tb(0.025%),Eu(1%)	594, 612, 617	143, 131, 106
C	$Sr_3Al_2O_6$:Tb(0.5%),Eu(0.025%)	420, 436, 446, 459, 485, 545, 551, 592, 615	81, 116, 101, 54, 69, 143, 91, 17, 14
D	$Sr_3Al_2O_6$:Tb(0.5%),Eu(0.1%)	468, 482, 544, 552, 592, 612, 616	53, 46, 50, 34, 28, 36, 32.
E	$Sr_3Al_2O_6$:Tb(0.025%),Eu(0.025%)	414, 430, 436, 468, 487, 496, 509, 540, 594, 601.	79, 177, 98, 77, 105, 95, 49, 52, 92, 53.

The emission spectra for the different concentration of dopant and co-dopant are shown in the figure 4.16. All the emission spectra were measured for the 254 nm excitation wavelength. The $Sr_3Al_2O_6$:Tb(0.025%), Eu (0.025%) shows peaks at 414, 430, 436, 468, 487, 496, 509, 540, 594 and 601 nm wavelength corresponding to the $^5D_3$ and $^5D_4$ transitions of Tb^{3+} as well as $^5D_0$ to $^7F_{1,2}$ transitions of Eu^{3+}. Only this system shows all the possible transitions of Tb^{3+} and Eu^{3+} in this system. The white light emission is also possible in this system when doped with appropriate amount of activator and co-activator.

The emission spectra for $Sr_3Al_2O_6$: Tb(0.5%), Eu (0.1%) shows the peaks at 468, 482, 544, 552, 592 , 612 and 616 nm when excited with the 254 nm wavelength. The transition from the $^5D_3$ level of Tb^{3+} is not clear but the main emission peak of Tb^{3+} (545 nm) becomes prominent in this phosphor. Also the emission of Eu^{3+} in the region 592, 612 and 616 has also increased. The reason behind the distortion of $^5D_3$ emission in this phosphor is may be the increase in the concentration of Eu^{3+}.

The emission spectra of $Sr_3Al_2O_6$:Tb(0.5%), Eu (0.025%) also show all the possible transition of Tb^{3+} whereas as the Eu^{3+} concentration is low the intensity of its emission is also low. From this phosphor it is evident that the distortion in the $^5D_3$ emission of Tb^{3+} in the above phosphor is caused due to the higher concentration of Eu^{3+}.

$Sr_3Al_2O_6$:Tb(0.025%), Eu(1%) shows the emission of Eu^{3+} only, while the $^5D_3$ as well as $^5D_4$ emission of Tb^{3+} is not observed in this phosphor.

The $Sr_3Al_2O_6$:Tb(0.1%), Eu(1%) shows emission at 545, 551, 593, 611 and 617 nm.
It is observed from the above study that when the co-activator concentration i.e. Eu^{3+} concentration is low, 0.025%, the $^5D3$ transition of Tb^{3+} becomes possible and the emission in the blue region is observed.

The addition of small amount of Eu^{3+} in the $Sr_3Al_2O_6$:Tb can forbid the cross-relaxation process of the Tb^{3+}. By adjusting the concentration of Tb^{3+} and Eu^{3+} in this system can allow to get the emission in all the ranges of the visible region.

4.5.4. Thermoluminescence glow curve of $Sr_3Al_2O_6:Tb^{3+},Eu^{3+}$ phosphor

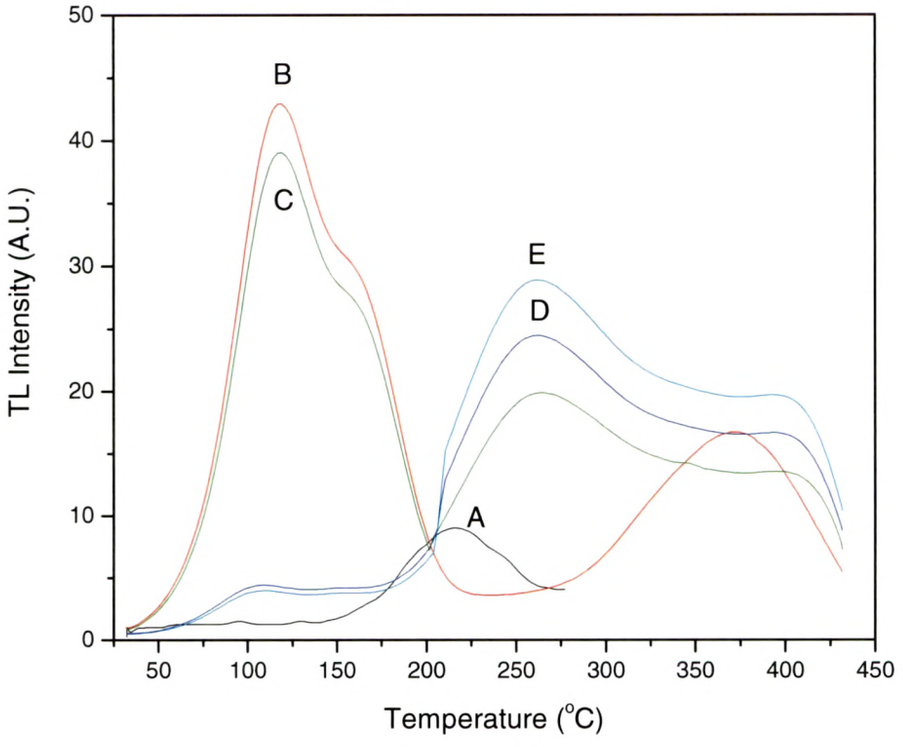

Figure 4.17. Thermoluminescence glow curve of $Sr_3Al_2O_6:Tb(1\%),Eu(x\%)$ phosphor for dose of 100 Gy from Sr-90, β source.
Curve A = $Sr_3Al_2O_6:Eu(1\%)$;
B = $Sr_3Al_2O_6:Tb(1\%)$;
C = $Sr_3Al_2O_6:Tb(1\%),Eu(0.025\%)$;
D = $Sr_3Al_2O_6:Tb(1\%),Eu(0.1\%)$;
E = $Sr_3Al_2O_6:Tb(1\%),Eu(0.5\%)$.

Table 4.7: Thermoluminescence peak intensity of $Sr_3Al_2O_6:Tb,Eu$ for varying concentration of Eu^{3+}.

Sample Code	$Sr_3Al_2O_6:Tb(x),Eu(y)$	TL peaks (°C)	TL Intensity (A.U.)
A	$Sr_3Al_2O_6:Eu(1\%)$	215	9
B	$Sr_3Al_2O_6:Tb(1\%)$	120, 163, 374	43, 30, 17
C	$Sr_3Al_2O_6:Tb(1\%),Eu(0.025\%)$	120, 162, 262, 350	39, 27, 20, 15
D	$Sr_3Al_2O_6:Tb(1\%),Eu(0.1\%)$	109, 262, 350	5, 25, 18
E	$Sr_3Al_2O_6:Tb(1\%),Eu(0.5\%)$	108, 262, 350	4, 29, 20

The energy transfer phenomenon in the $Sr_3Al_2O_6$:Tb,Eu phosphor can also be observed using the thermoluminescence studies. Figure 4.17. shows the thermoluminescence glow curve of the $Sr_3Al_2O_6$:Tb,Eu phosphor, where the concentration of Eu^{3+} increased gradually whereas the concentration Tb^{3+} kept constant at 1%. For comparison the glow curve of $Sr_3Al_2O_6$:Eu (1%) is also shown in the figure. The curve of $Sr_3Al_2O_6$:Eu(1%) shows the single low intensity peak at around 215 °C, whereas the glow peak of $Sr_3Al_2O_6$:Tb(1%) shows peaks around 124, 164 and 340 °C. The addition of Eu^{3+} in $Sr_3Al_2O_6$:Tb(1%) changes the glow curve.

The thermoluminescence glow curve of $Sr_3Al_2O_6$:Tb(1%), Eu(0.025%) shows the peaks around 124, 164 and 262 °C. The intensity of the 124 and 164 °C peaks also decreases by small amount. A new peak at 262 °C is observed on addition of Eu^{3+}. The well defined and prominent peak of 340 °C changes into the shoulder of the 262 °C peak. The 262 °C peak in this system shows the formation of new traps. The glow curve of $Sr_3Al_2O_6$:Tb(1%), Eu(0.1%) shows that the peak of 124 and 164 °C has been reduced remarkably and the TL intensity of the 262 °C peak increases with small intensity. Further increase in the Eu^{3+} concentration to 0.5% doesn't affect much to the intensity of 124 and 164 °C peaks as it has already less intensity, but it helps to improve the intensity of the 262 °C peak.

The increase in the Eu^{3+} concentration decreases the main TL dosimetric peak of Tb^{3+} i.e., 124 and 164 °C peak.

This suggests that the Eu^{3+} act as a quencher in the system. The 262 °C is also not stable and reduces drastically within 48 hours. The $Sr_3Al_2O_6$:Tb, Eu system cannot be considered as a dosimetric phosphor.

4.5.5. Thermoluminescence glow curve of $Sr_3Al_2O_6:Tb^{3+},Eu^{3+}$ phosphor with varying concentration of Tb^{3+} and Eu^{3+}

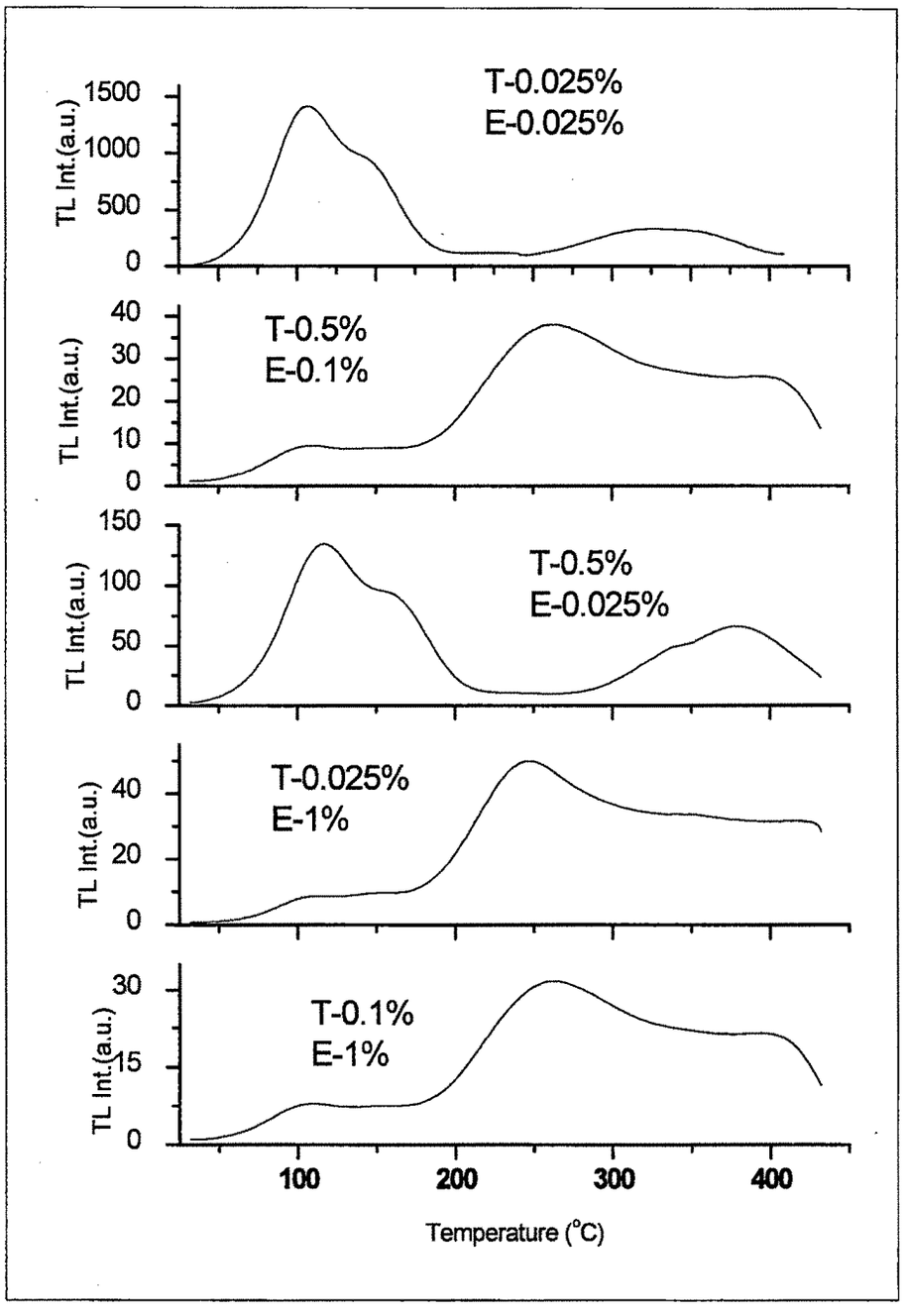

Figure 4.17. Thermoluminescence glow curve of $Sr_3Al_2O_6:Tb,Eu$ phosphor for dose of 100 Gy from ^{90}Sr β source. The concentration of Tb^{3+} and Eu^{3+} is varying and indicated on the respective glow curve. Where T = Tb^{3+} and E = Eu^{3+}.

Table 4.8: Thermoluminescence peak intensity of $Sr_3Al_2O_6$:Tb,Eu for varying concentration of Tb^{3+} and Eu^{3+}.

Sample Code	$Sr_3Al_2O_6$:Tb(x),Eu(y)	TL peaks (°C)	TL Intensity (A.U.)
A	$Sr_3Al_2O_6$:Tb(0.1%),Eu(1%)	113, 261, 350	8, 32, 22
B	$Sr_3Al_2O_6$:Tb(0.025%),Eu(1%)	105, 245, 340	9, 50, 33
C	$Sr_3Al_2O_6$:Tb(0.5%),Eu(0.025%)	118, 162, 382	132, 93, 63
D	$Sr_3Al_2O_6$:Tb(0.5%),Eu(0.1%)	108, 261, 350	10, 35, 27
E	$Sr_3Al_2O_6$:Tb(0.025%),Eu(0.025%)	106, 145, 329	1400, 987, 353

The effect of different concentration of activator (Tb^{3+}) and co-activator (Eu^{3+}) on the TL glow curve of $Sr_3Al_2O_6$:Tb, Eu was studied. The TL measurement of five sets of varying concentration of Tb^{3+} and Eu^{3+} were performed as shown in the figure 4.17. The TL glow curve of $Sr_3Al_2O_6$:Tb(0.025%), Eu(0.025%) shows peak around 124, 164 and 340 °C with very high intensity. Also the TL dosimetric peak 164 °C of this phosphor shows all the characteristics of the dosimetric peak and also show less fading when stored in dark for around two months. The PL spectra of this phosphor also show emission in all ranges of the visible region. Hence this phosphor can be considered as a good candidate for lamp phosphor as well as dosimetric purpose.

The TL glow curve of $Sr_3Al_2O_6$:Tb(0.5%), Eu(0.1%) shows the peaks around 124, 262 °C along with the peak of 340 °C turns into a shoulder. Increase in the Eu^{3+} is responsible for the reduction in the intensity of 124 ad 164 °C peak. Whereas the small amount of Eu^{3+} concentration is responsible for decrease in the intensity of 124, 164 and 340 °C peak only, as shown in the glow curve of $Sr_3Al_2O_6$:Tb(0.5%), Eu(0.025%).

The glow curves of $Sr_3Al_2O_6$:Tb(0.025%), Eu(1%) and $Sr_3Al_2O_6$:Tb(0.1%), Eu(1%) shows the effect of increase in the Tb^{3+} concentration on the glow curve. From the figure 4.17. it is noted that the increase in the Tb^{3+} concentration reduces the intensity of the 262 °C glow peak.

Thus from all the above discussion it is clear that only the $Sr_3Al_2O_6$:Tb(0.025%), Eu(0.025%) only fulfills the characteristics of dosimetry as well as lamp phosphor.

4. 6. References

[1] E. Bulur, H.Y. Goksu, A. Wieser, M. Figel, A.M. Ozer, Radiat. Prot. Dosim. 65 (1996) 373.

[2] S.-M. Yeh, C.S. Su, Radiat. Prot. Dosim. 65 (1996) 359.

[3] R.A. Rodriguez, E. De la Rosa, R. Melendrez, P. Salas, J. Castaneda, M.V. Felix, M. Barboza-Flores, Opt. Mater. 27 (2005) 1240.

[4] R.A. Rodriguez, E. De la Rosa, L.A. Diaz-Torres, P. Salas, R. Melendrez, M. Barboza-Flores, Opt. Mater. 27 (2004) 293.

[5] R.A. Rodriguez-Rojas, E. De la Rosa-Cruz, L.A. Diaz-Torres, P. Salas, R. Melendrez, M. Barboza-Flores, M.A. Meneses-Nava, O. Barbosa-Garcia, Opt. Mater. 25 (2004) 85.

[6] L. Liu, Y. Zhang, J. Hao, C. Li, Q. Tang, C. Zhang, Q. Su, Physica status solidi (a) 202 (2005) 2800.

[7] K.V.R. Murthy, Y.S. Patel, A.S. Sai Prasad, V. Natarajan, A.G. Page, Radiat. Measurements 36 (2003) 483.

[8] K.V.R. Murthy, S.P. Pallavi, R. Ghildiyal, M.C. Parmar, Y.S. Patel, V. Ravi Kumar, A.S. Sai Prasad, V. Natarajan, A.G. Page, Radiat. Prote. Dosim. 120 (2006) 238.

[9] T. Katsumata, R. Sakai, S. Komuro, T. Morikawa, J. Electrochem. Soc. 150 (2003) H111.

[10] D. Wang, Y. Li, Y. Xiong, Q. Yin, J. Electrochem. Soc. 152 (2005) H12.

[11] P. Page, R. Ghildiyal, K.V.R. Murthy, Mater. Res. Bull. 41 (2006) 1854.

[12] M. Akiyama, C. Xu, Y. Liu, K. Nonaka, T. Watanabe, J. Lumin. 97 (2002) 13.

[13] Pallavi Page, Rahul Ghildiyal, K.V.R. Murthy, Materials Research Bulletin 43 (2008) 353–360

[14] JCPDS-ICDD Card No. 24-1187.

[15] A.K. Prodjosantoso, B.J. Kennedy, B.A. Hunter, Aust. J. Chem. 53 (2000) 195.

[16] A Potdevin, Chadeyron, D Boyer, B Caillier and R Mahiou, J. Phys. D: Appl. Phys. 38 (2005) 3251–3260

[17] G. Wakefield, H.A. Keron, P.J. Dobson, J.L. Hutchison, J. Phys. Chem. Solids 60 (1999) 503.

[18] G.H. Dieke, Spectra and Energy Levels of Rare Earth Ions in Crystals, Wiley, 1968 p. 138.

[19] P.A.M. Berdowski, M.J.J. Lammers, G. Blasse, Chem. Phys. Lett. 113 (1985) 387.

[20] J.P. Van der Ziel, L. Kopf, L.C. Van Uitert, Phys. Rev. B 6(1972) 615.

[21] M.J. Weber, Phys. Rev. B 4 (1971) 2932.

[22] Yun Liu and Chao-Nan Xu, J. Phys. Chem. B 107 (2003) 3991.

[23] S.W.S. Mckeever, Thermoluminescence of Solids, Cambridge University Press, Cambridge, 1985, p. 205.

[24] R. Chen, Y. Kirsh, Analysis of Thermally Stimulated Processes, Pergamon Press, Oxford, 1981, p. 159.

[25] K.S.V. Nambi, V.N. Bapat, A.K. Ganguly, Journal of Physics C 7 (1974) 4403.

[26] S. Chatterjee, V. Shanker, H. Chander, Mater. Chem. Phys. 80 (2003) 719.

[27] D.L. Dexter, J. Chem. Phys. 21 (1953) 836.

[28] G. Blasse. Luminescent Materials, Springer, Berlin (1994) 93.

[29] Kee-Sun Sohn, Fung suk Park, Chang Hae Kim and Hee Dong Park, J. Electrochem. Soc., 147 (11) (2000) 4368.